CHAPTER IV

SPATIOTEMPORAL ANALYSIS OF POPULATION GENETIC STRUCTURE IN *GEOMONHYSTERA DISJUNCTA* (NEMATODA, MONHYSTERIDA) REVEALS HIGH LEVELS OF MOLECULAR DIVERSITY

ABSTRACT

Species identification in the phylum Nematoda is complicated due to the paucity of easily obtainable diagnostic morphological features. Furthermore, the cosmopolitan distribution of several species despite low dispersal abilities makes cryptic diversity potentially substantial within this phylum. We conducted a population genetic survey in the marine nematode *Geomonhystera disjuncta* in Belgium and The Netherlands in two seasons. The mitochondrial cytochrome oxidase c subunit 1 (COI) gene was screened with the single-strand conformation polymorphism method in 759 individuals. The 43 haplotypes were grouped into five lineages, with low divergences within (< 3%) and high divergences between lineages (> 14%). Analysis of the nuclear ITS region yielded concordant tree topologies, indicating the presence of five cryptic taxa within *G. disjuncta*. Analysis of Molecular Variance (AMOVA) illustrated a significant structuring in all lineages and temporal fluctuations in haplotype frequencies within and between locations. Metapopulation dynamics and/or priority effects best explained this structuring. Finally, our data indicate that the COI gene may be useful for DNA barcoding purposes.

INTRODUCTION

Nematodes are one of the most abundant and diverse metazoan phyla in terms of species richness (Lambshead 2004), comprising both parasitic and free-living species. Only a small fraction of the total predicted nematode diversity is currently described (e.g. Hugot et al. 2001, Blaxter et al. 2005), mainly due to their small body size (~ 1 mm). This complicates species identification because important morphological features may be situated at scales that are beyond the resolution of light microscopy (Coomans 2002, De Ley et al. 2005, Markmann & Tautz 2005). In addition, many nematode species have a worldwide distribution, despite an endobenthic life style, a lack of pelagic larvae and a limited dispersal capacity. Obviously, the combined effects of morphological limitations in species identification and a cosmopolitan distribution despite limited dispersal abilities make cryptic diversity potentially substantial within the Nematoda.

Population genetic surveys provide important information on genetic diversity within and connectivity between populations and frequently uncover cryptic taxa (Schizas et al. 1999, Knowlton 2000, Rocha Olivares et al. 2001, Govindarajan et al. 2005). In this way, they have challenged the longstanding view of low species diversity and broad-scale homogeneity in the marine environment (Caudill & Bucklin 2004, Ovenden et al. 2004). Within the Nematoda, population genetic studies have mainly been restricted to parasitic species (e.g. Blouin et al. 1995, Hu et al. 2002, Hoglund et al. 2004, Picard et al. 2004 but see Sivasundar & Hey 2005). The single free-living marine species hitherto studied, *Pellioditis marina*, showed restricted gene flow and cryptic diversity even on a very local scale (40 km), which was at variance with expectations based on this species' potentially substantial passive dispersal capacity and its life-history characteristics (Derycke et al. 2005, 2006). In addition, cytochrome oxidase c subunit I (COI) and ribosomal intergenic transcribed spacer (ITS) data unravelled four cryptic taxa within *P. marina*, with sequence divergences between them ranging from 5.8 - 10.6 % for COI and 3.3 – 21.1 % for ITS. These high divergences raise questions on the modes of speciation and on the generality of such cryptic diversity in other marine nematodes occurring in areas with supposedly well-described nematode communities. Indeed, recent diversity assessments in the marine environment based on DNA barcoding indicate that cryptic diversity is far more common than initially thought (Blaxter 2004).

The major objective of the present study is to analyse the population genetic structure of a second marine nematode species, *Geomonhystera disjuncta* (Bastian, 1865)[19] (Monhysteridae), as a first step towards inferring more general conclusions on population genetic structuring and cryptic diversity in free-living marine nematodes. The genus *Geomonhystera* Andrássy, 1981 differs from the other monhysterid genera in the position of the vulva, which is typically situated far back, at more than 75 % of the body length (Andrássy 1981). The genus contains 15 valid species, seven of which are marine (Jacobs 1987). *G. disjuncta* can be distinguished from the other six by differences in body size, position of the vulva, shape and length of the tail, and shape and number of eggs (De Coninck & Schuurmans Stekhoven 1933, Hopper 1969). The sampling area – which is well-investigated with respect to its nematode communities (e.g. Vincx 1990, Vincx et al. 1990) – and design were similar to those for *P. marina* (Derycke et al. 2005), except that we sampled in two different seasons. *G. disjuncta* occurs sympatrically with *P. marina* and also has a short generation time (ca. 8 days) with a high reproductive output (ca 200-500 eggs female^{-1}) (Vranken et al. 1988). However, *G. disjuncta* differs from *P. marina* in several other aspects of its life-history characteristics: 1) it does not produce Dauerlarvae (i.e. metabolically less active larvae that can survive unfavourable conditions) (Bongers & Bongers 1998); 2) it occurs under a broader range of food (bacteria) availability (Vranken et al. 1988, Moens & Vincx 2000); and 3) it is not solely found on macroalgal detritus, but also on other organic materials (Mokievsky et al. 2005) and in marine sediments (Heip et al. 1985, Vranken 1987).

In view of these characteristics, two main aims were targeted in this study: 1) to investigate the population genetic structure of *G. disjuncta* and compare it with that of *P. marina*, a sympatrically occurring nematode species with different life-history characteristics; and 2) to assess intraspecific diversity and possible cryptic taxa in *G. disjuncta* by using different molecular markers and phylogenetic analyses.

---

[19] See General Introduction, p 9: *Geomonhystera disjuncta* is recently renamed to *Halomonhystera disjuncta*. *Pellioditis* is now considered a subgenus of *Rhabditis*.

MATERIAL AND METHODS

SAMPLE COLLECTION AND PROCESSING

We sampled *Geomonhystera disjuncta* at eight locations along the Belgian coast and southwestern part of The Netherlands (Fig. 4.1). Nematodes were collected from *Fucus sp.* fragments at four estuarine locations in the Westerschelde (Br, Pa, Ze and Kr), two coastal locations in Belgium (Ni and Bl), and one location in the Oosterschelde (Os, a coastal lagoon). In addition, we collected *G. disjuncta* from *Ulva sp.* and *Enteromorpha sp.* in Lake Grevelingen (Gr), as *Fucus sp.* was not found there. For a more detailed description of the locations and collection methods we refer to Derycke et al. (2006). This geographical sampling scheme was conducted in April 2003 and repeated in January 2004. Additional samples were collected in Br in summer 2003, and in Os and Gr in autumn 2003.

We incubated randomly collected fragments of algal thalli on agarslants for a maximum of five days. This period is shorter than the shortest generation time of *G. disjuncta* (Vranken et al. 1988, Moens unpubl.) under optimal conditions, and hence ensured that we sampled the natural population rather than individuals bred in the laboratory. Adult *G. disjuncta* were identified alive under a dissecting microscope using morphological and behavioral characteristics, handpicked and transferred to sterile water. Because of its small body size (less than 1.5 mm), and because of limits to the diagnostic power of the characteristics that can be observed on live individuals, we created an identification backup as follows: 80 - 100 individuals from each location were transferred into one embryo dish containing sterile artificial seawater with a salinity of 25; 50 of these were randomly picked out and preserved on acetone (ca. 70 - 95 %) for molecular analysis. The remaining individuals were mounted on glycerine slides (Vincx 1996), and subsequently identified at high magnification under a microscope (Leica DLMB; magnification 100X) using species descriptions (De Coninck & Schuurmans Stekhoven 1933, Gerlach 1965, Hopper 1969, Warwick et al. 1998). In addition, we performed morphometric analysis on a subset of individuals belonging to different mitochondrial lineages (throughout the manuscript, we use the term 'lineage' to refer to the highly divergent haplotype groups shown in Fig. 4.4): 10 randomly chosen individuals (five males and five females) from each of

Fig. 4.1: *Geomonhystera disjuncta*. Distribution of the five lineages (Gd1, Gd2, Gd3, Gd4 and Gd5) among the eight sampled locations in Belgium and The Netherlands. The stacked column diagrams show the percentage of each lineage during spring (sp), summer (su), and autumn (au) 2003 and winter 2004 (wi) in each location. The summer and autumn campaign were only successful for 1 and 2 locations respectively. No *G. disjuncta* specimens were found in the upstream Westerschelde locations (Ze and Kr) nor in Lake Grevelingen (Gr) in the summer campaign. All other sampling gaps are due to a very low PCR success rate. Ni = Nieuwpoort; Bl = Blankenberge; Br = Breskens; Pa = Paulina; Ze = Zeedorp; Kr = Kruispolderhaven; Os = Oosterschelde; Gr = Grevelingen.
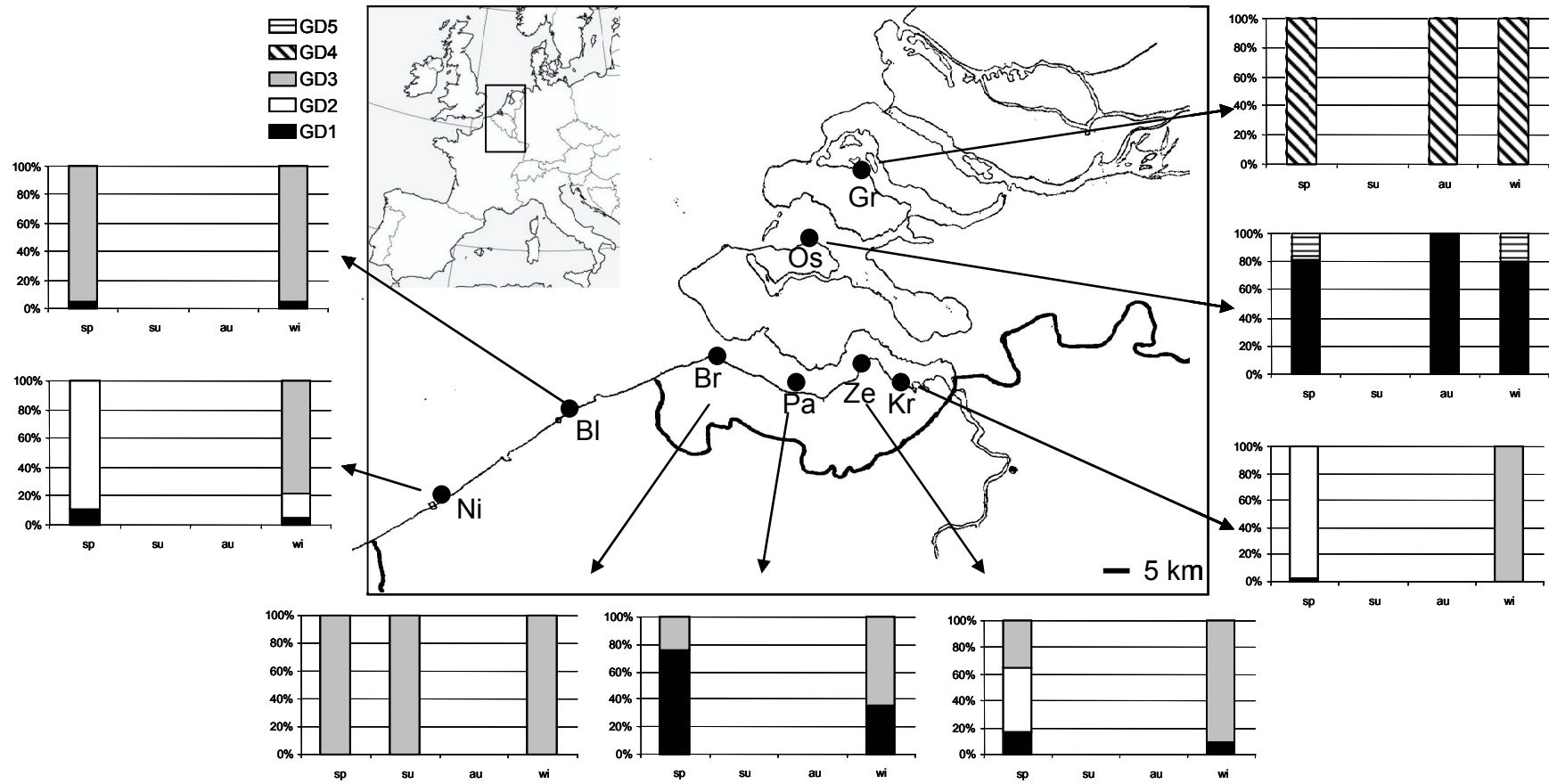
four localities containing a single lineage (Gr and Br) or nearly so (i.e. ≥ 98 % of all individuals belong to the same lineage, Kr and Os) were processed[20]. Glycerine slides were mounted under a Leitz Dialux 20 microscope (magnification 10X25X and 10X50X), and a Sanyo CCD video camera and the Quantimet 500 software were used for measurements. We measured total body length (L) and maximum body width (mbd). Additional parameters were anal body diameter (abd) and length of spicules (spic) for males, and distance between vulva-mouth (v) and between vulva-anus in females. Three ratios were calculated: L/mbd, spic/abd, %V. This procedure enabled us to exclude misidentifications during the first step of the nematode isolation method.

MOLECULAR ANALYSIS

We screened approximately 40 individuals from each location and time for variation in the mitochondrial DNA COI gene, except for Ni in January 2004, where *n* = 23. For a detailed description of the DNA extraction protocol we refer to Derycke et al. (2005). After DNA preparation, 422 bp of the COI gene were amplified with the following degenerated primers: JB2 (5'- ATGTTTTGATTTTACCWGCWTTYGG TGT–3') and JB5GED (5'–AGCACCTAAACTTAAAACATARTGRAARTG – 3')[21]. All populations collected in April were analysed with this primer set. However, PCR-amplification of individuals from Os and Gr collected in autumn 2003 and winter 2004 was problematic. Therefore, we designed a new degenerated reverse primer (JB8: 5'-CCCCTCTAGTCTWCTATTTCTTAATAC–3') located 29 bp upstream of the 30 bp long JB5GED primer, yielding a fragment of 363 bp. PCR conditions were as in Derycke et al. (2005), except for the annealing temperature, which was 50°C for both primersets. Variation in the COI gene was detected using the Single Strand Conformation Polymorphism (SSCP) method as described in Derycke et al. (2005). We sequenced all PCR-products with different SSCP-profiles with the aforementioned primers (accession numbers AM180357 – AM180399), as were 10 % of all individuals in every location to confirm the agreement between SSCP-band

---

[20] Morphological and molecular data were collected from different specimens. The link between molecular lineages and morphometric data was established by analysing specimens from localities where only one (or nearly so) molecular lineage was encountered.
[21] The remaining DNA was stored at -80°C. In this way, multiple loci could be amplified from the same individual.

mobility and sequence variation. PCR products were purified and sequenced as described in Derycke et al. (2005).

COI haplotypes were grouped into five highly divergent lineages (Fig. 4.4). Three individuals of each lineage, representing the three most abundant haplotypes of that lineage, were sequenced for the nuclear ribosomal ITS1 - 5.8S - ITS2 region. In addition, we sequenced two individuals containing haplotype G61. The ITS region was amplified and sequenced as in Derycke et al. (2005) (accession numbers AM180400 – AM180415).

DATA ANALYSIS

Statistical analysis of morphometric data.

The primary objective of the measurements was to ensure that all specimens were *G. disjuncta*. However, the same data allow a first exploration of whether morphological differences between the genetic lineages exist. The data met the assumptions of normality and homoscedasticity, and analysis of variance (ANOVA) and Tukey's HSD pairwise comparisons (Statistica 6.0, Statsoft 2001) were used to assess whether morphological differences occurred between the mitochondrial DNA lineages.

COI variation and phylogenetic analysis.

COI sequences were aligned in ClustalX v.1.74 (Thompson et al. 1997). The number of pairwise differences between all haplotypes was calculated in Mega 3.0 (Kumar et al. 2004). A statistical parsimony network was constructed in TCS v.1.18 (Clement et al. 2000) to explore the evolutionary relationships among haplotypes. This yielded several unconnected subnetworks, indicating that some haplotypes were too divergent to establish a reliable parsimonious connection (i.e. 95 %). The aligned sequences were used for further phylogenetic analysis in PAUP* 4.0 beta 10 (Swofford 1998).

The ITS alignment was constructed in ClustalX v 1.74 (Thompson et al. 1997) with default gap costs. Several indels were observed, and ambiguous sites were improved manually in Genedoc 2.6 (Nicholas & Nicholas 1997). Modeltest 3.7 (Posada & Crandall 1998) and the Akaike Information Criterion (Posada & Buckley 2004) were used to determine the maximum likelihood settings for constructing the

neighbour - joining (NJ) tree: the HKY+I+G model (Hasegawa et al. 1985) gave the best fit for the COI fragment and for the simultaneous analysis of COI and ITS. A permutation homology test (Mickevich & Farris 1981) was performed using PAUP* to assess the degree of phylogenetic incongruence between COI and ITS data. Parsimony (MP) trees were obtained using a random stepwise addition of sequences and a tree-bisection-reconnection branch swapping algorithm (with 10000 rearrangements). Bootstrap values for MP and NJ were inferred from 1000 replicates. In addition, a Bayesian analysis was performed in MrBayes v 3.1.2 (Huelsenbeck & Roncquist 2005). Four independent Markov chains were run for 500 000 generations, with a tree saved every 10th generation. The first 10 000 trees were discarded as burn-in. MrModeltest 2.2 (Nylander 2004) was used to determine the best model for Bayesian analysis of our data: the HKY+I+G model best fitted the COI fragment, while the HKY+I model was chosen for the ITS data.

Population genetic structure (COI).

Intra-populational diversity was assessed by calculating haplotype - (h, Nei 1987) and nucleotide diversity (π, Nei 1987) in Arlequin v.2.0 (Schneider et al. 2000). Both parameters were tested for significant differences between mitochondrial lineages and between locations within lineages by a non-parametric Kruskal–Wallis test. Pairwise a posteriori comparisons were performed with the Mann–Whitney U test, corrected by the sequential Bonferroni method (Rice 1989). The statistical tests were performed with the Statistica 6.0 program (Statsoft 2001).

Heterogeneity between populations was investigated with an analysis of molecular variance (AMOVA) as implemented in Arlequin v 2.0. The total dataset was divided such that genetic structure was analysed for each lineage and at each time point separately by a single–level AMOVA (i.e. without nesting). This analysis could not be performed for Gd4 and Gd5, as these lineages were restricted to a single locality. The isolation-by-distance model was tested with IBD 1.5 (Bohonak 2002) for those lineages occurring in several locations at both time points (Gd1 and Gd3). Geographic distance between populations was measured as the shortest continuous water surface distance, and was compared with Cavalli-Sforza & Edwards' (1967) chord distances (DCE) between populations.

Temporal analysis of the population genetic structure.

No temporal analysis of the genetic structure was performed for lineage Gd2 as it only occurred at one location (Ni) in January 2004 (Fig. 4.1). Stability of the observed genetic patterns over time in lineages Gd1 and Gd3 was tested in two different ways. First, significant differences in the level of spatial genetic variation (Fst) for Gd1 and Gd3 in 2003 and 2004 were tested with a randomisation procedure (10,000 permutations) as implemented in Fstat v 2.9.3 (Goudet 2001). Secondly, Cavalli-Sforza & Edwards' (1967) chord distances (DCE) for Gd1 and Gd3 were calculated between populations within each year using Phylip 3.6 (Felsenstein 2004). This yielded two matrices (spring 2003 and winter 2004) with genetic distances for each lineage. These matrices were compared by a Mantel test with 1000 permutations as implemented in TFPGA 1.3 (Miller 1997). A significant test result indicates that genetic distances between localities are correlated and thus that the degree of genetic structure remains stable over time. Finally, spatial and temporal differentiation were compared in a two-level AMOVA (i.e. temporal samples were pooled within localities) for both lineages. Temporal changes in haplotype frequencies within every locality were investigated for all five lineages separately using a single-level AMOVA.

RESULTS

MORPHOMETRIC DATA

Male body length varied between 0.84 and 1.40 mm, while female body length ranged between 0.87 and 1.33 mm. No significant differences were observed between lineages (p = 0.35 for males and p = 0.52 for females). Maximum body width in females ranged from 31.86 – 49.15 μm and from 26.8 – 42.1 μm in males, which resulted in lower values of the female L/mbd ratio (Fig. 4.2a). Total body width was similar for all lineages (p = 0.91 for males and p = 0.45 for females). No significant differences in measurements were found among females when allocated to genetic lineages: e.g. %V ranged from 84.35 % to 93.22 % (p = 0.1). Although spicule length (ranging from 32.35 – 41.26 μm) and abd (ranging from 21.09 – 29.87) were not significantly different between lineages (p = 0.29 and p = 0.11 respectively), the spic/abd ratio was different between males from lineages Gd2 and Gd3 (p = 0.01, Fig. 4.2b).

A

B
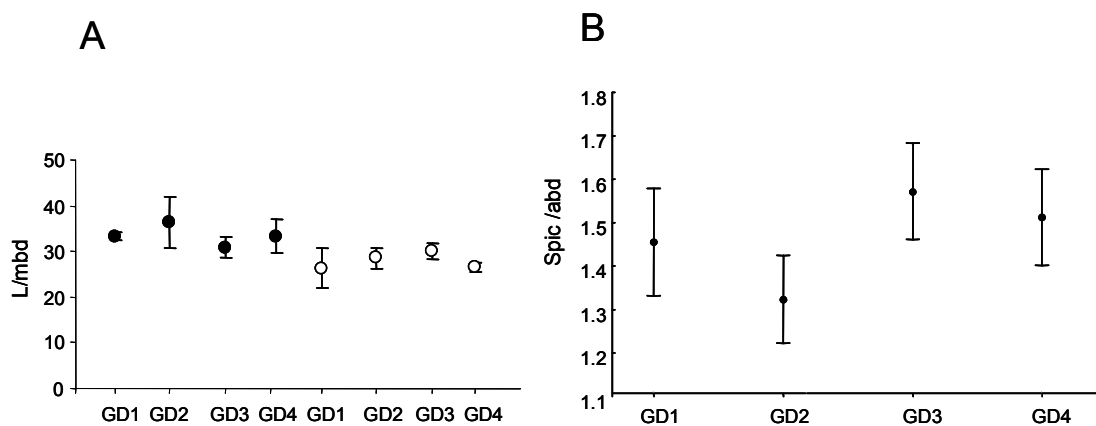
Fig. 4.2: *Geomonhystera disjuncta*. Morphometric data of specimens belonging to lineages Gd1, Gd2, Gd3 and Gd4, respectively. A: L/mbd ratio of males (black dots) and females (white dots); B: spic/abd ratio of males. Each dot represents the average of measurements in five specimens, and error bars represent standard deviations. Current effect: $F_{(3, 16)}= 4.61$, $p = 0.017$.

COI VARIATION

A total of 311bp of the COI gene was screened in 759 individuals of *G. disjuncta* (Table 4.1). This fragment contained 117 variable positions, 112 of which were parsimony informative and five of which were singletons. This yielded 43 different haplotypes, with divergences among haplotypes ranging from 0.32 –

25.72 % (1 – 80 substitutions). This corresponded with 0 – 6 amino acid changes. No indels occurred in the alignment. The parsimony network contained six unconnected subnetworks, indicating that high levels of divergence were present between these haplotype groups (the distinction between Gd1, 2, 3, 4a, 4b and 5 is based on the phylogenetic analysis (see next section); Fig. 4.3). For clarity, these haplotype groups will be referred to as lineages in what follows. The number of substitutions between haplotypes of a particular lineage was low and ranged from 0.32 – 2.56 % (but see end of next section), while high divergences were observed between haplotypes of different lineages (13.8 – 25.7 %).
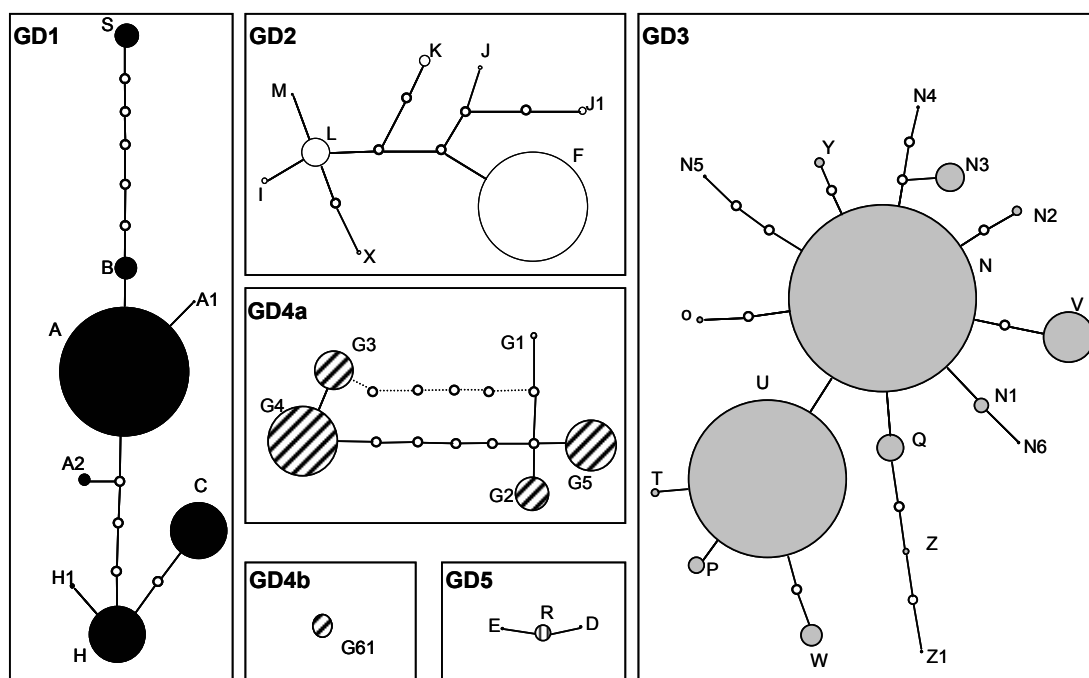
Fig. 4.3: *Geomonhystera disjuncta.* Statistical parsimony network among 42 COI haplotypes (haplotype D1 is missing due to incomplete sequence information). Shadings are in agreement with the lineages presented in Fig. 4.1. Circles are proportional to the absolute frequency of haplotypes in the total dataset. Small white circles are missing haplotypes.

Lineage Gd3 was highly diverse and contained 17 haplotypes, which are connected to each other via a starlike pattern. Haplotypes N and U occurred in high frequency while most other haplotypes were rare (Fig. 4.3). In fact, these two haplotypes were the most abundant and widespread haplotypes: they were present in each locality, except for Gr and Os. Gd1 and Gd4a contained few rare haplotypes and are characterized by many missing haplotypes. Gd4b consisted of a single haplotype (G61), and this haplotype contained four of the five observed singletons. Like all haplotypes of Gd4a, haplotype G61 only occurred in Gr. A starlike pattern was also present in haplotype group Gd2. Interestingly, the most frequently observed

Table 4.1. *Geomonhystera disjuncta*. Haplotype frequencies for the eight populations during four sampling events. Haplotypes are arranged by lineage (Gd1-5). (n) number of individuals; (h) haplotype diversity; (π) nucleotide diversity. Sample abbreviations as in Fig. 4.1. Accession numbers of each haplotype are also indicated.

GD1

Season	Pop	A	A1	A2	B	C	S	H	H1	n	h	π
Spring	Ze	1	0	0	0	2	0	4	0	7	0.667	0.007
Spring	Kr	0	0	0	0	1	0	0	0	1	na	na
Spring	Pa	5	0	0	0	0	6	21	0	32	0.526	0.010
Spring	Br	0	0	0	0	0	0	0	0	0	-	-
Spring	Os	11	0	0	9	10	3	1	0	34	0.752	0.013
Spring	Bl	0	0	0	0	0	2	0	0	2	na	na
Spring	Ni	3	0	0	1	0	0	0	0	4	0.500	0.010
Spring	Gr	0	0	0	0	0	0	0	0	0	-	-
Summer	Br	0	0	0	0	0	0	0	0	0	-	-
Autumn	Os	22	0	3	0	10	0	5	3	43	0.677	0.010
Autumn	Gr	0	0	0	0	0	0	0	0	0	-	-
Winter	Ze	3	0	0	0	0	0	0	0	3	na	na
Winter	Kr	0	0	0	0	0	0	0	0	0	-	-
Winter	Pa	11	0	0	0	0	3	0	0	14	0.363	0.008
Winter	Br	0	0	0	0	0	0	0	0	0	-	-
Winter	Os	18	2	4	4	9	0	0	0	37	0.697	0.009
Winter	Bl	0	0	0	0	0	2	0	0	2	na	na
Winter	Ni	1	0	0	0	0	0	0	0	1	na	na
Winter	Gr	0	0	0	0	0	0	0	0	0	-	-
Total		75	2	7	13	33	14	33	3	180		
Accession number		AM180357	AM180369	AM180370	AM180358	AM180359	AM180372	AM180396	AM180389			

GD2

Season	Pop	F	I	J	J1	K	L	M	X	n	h	π
Spring	Ze	16	3	0	2	0	0	0	0	21	0.410	0.008
Spring	Kr	26	0	3	3	0	10	0	3	45	0.332	0.006
Spring	Pa	0	0	0	0	0	0	0	0	0	-	-
Spring	Br	0	0	0	0	0	0	0	0	0	-	-
Spring	Os	1	0	0	0	0	0	0	0	1	na	na
Spring	Bl	0	0	0	0	0	0	0	0	0	-	-
Spring	Ni	21	1	0	0	7	3	2	0	34	0.581	0.007
Spring	Gr	0	0	0	0	0	0	0	0	0	-	-
Summer	Br	0	0	0	0	0	0	0	0	0	-	-
Autumn	Os	0	0	0	0	0	0	0	0	0	-	-
Autumn	Gr	0	0	0	0	0	0	0	0	0	-	-
Winter	Ze	0	0	0	0	0	0	0	0	0	-	-
Winter	Kr	0	0	0	0	0	0	0	0	0	-	-
Winter	Pa	0	0	0	0	0	0	0	0	0	-	-
Winter	Br	0	0	0	0	0	0	0	0	0	-	-
Winter	Os	0	0	0	0	0	0	0	0	0	-	-
Winter	Bl	0	0	0	0	0	0	0	0	0	-	-
Winter	Ni	0	0	0	0	4	0	0	0	4	na	na
Winter	Gr	0	0	0	0	0	0	0	0	0	-	-
Total		64	4	3	5	7	17	2	3	105		
Accession number		AM180362	AM180390	AM180371	AM180386	AM180392	AM180391	AM180393	AM180376			

GD3

Season	Pop	N	N1	N2	N3	N4	N5	N6	O	P	Q	T	U	V	W	Y	Z	Z1	n	h	π
Spring	Ze	3	0	0	0	0	0	0	6	0	2	0	0	4	0	0	0	0	15	0.762	0.005
Spring	Kr	0	0	0	0	0	0	0	0	0	0	0	0	0	0	0	0	0	0	-	-
Spring	Pa	7	0	0	0	0	0	0	3	0	0	0	0	0	0	0	0	0	10	0.467	0.002
Spring	Br	5	8	0	0	0	0	0	3	10	6	7	0	0	0	0	0	0	39	0.835	0.007
Spring	Os	0	0	0	0	0	0	0	0	0	0	0	0	0	0	0	0	0	0	-	-
Spring	Bl	16	0	0	0	0	0	4	8	0	3	7	0	0	0	0	0	0	38	0.747	0.004
Spring	Ni	0	0	0	0	0	0	0	0	0	0	0	0	0	0	0	0	0	0	-	-
Spring	Gr	0	0	0	0	0	0	0	0	0	0	0	0	0	0	0	0	0	0	-	-
Summer	Br	10	0	0	0	0	0	2	0	0	0	2	10	10	1	0	4	0	39	0.807	0.007
Autumn	Os	0	0	0	0	0	0	0	0	0	0	0	0	0	0	0	0	0	0	-	-
Autumn	Gr	0	0	0	0	0	0	0	0	0	0	0	0	0	0	0	0	0	0	-	-
Winter	Ze	18	0	2	0	0	0	0	0	0	0	7	3	1	0	0	0	0	31	0.671	0.004
Winter	Kr	3	0	0	4	0	0	0	0	5	0	19	2	2	0	0	0	0	35	0.677	0.005
Winter	Pa	9	0	3	0	2	0	0	0	0	0	12	0	0	0	0	0	0	26	0.674	0.004
Winter	Br	23	0	0	0	0	2	0	0	0	2	6	8	1	0	0	0	0	42	0.654	0.004
Winter	Os	0	0	0	0	0	0	0	0	0	0	0	0	0	0	0	0	0	0	-	-
Winter	Bl	7	0	0	13	0	0	0	0	2	0	11	0	1	0	0	2	0	36	0.752	0.006
Winter	Ni	8	1	1	0	0	0	0	0	0	0	5	3	0	0	0	0	0	18	0.732	0.003
Winter	Gr	0	0	0	0	0	0	0	0	0	0	0	0	0	0	0	0	0	0	-	-
Total		109	9	6	17	2	2	4	10	16	5	92	30	13	6	4	2	2	329		
Accession number		AM180379	AM180381	AM180384	AM180383	AM180385	AM180387	AM180388	AM180394	AM180395	AM180397	AM180373	AM180374	AM180378	AM180377	AM180375	AM180380	AM180382			

GD4

Season	Pop	G1	G2	G3	G4	G5	G61	n	h	π
Spring	Ze	0	0	0	0	0	0	0	-	-
Spring	Kr	0	0	0	0	0	0	0	-	-
Spring	Pa	0	0	0	0	0	0	0	-	-
Spring	Br	0	0	0	0	0	0	0	-	-
Spring	Os	0	0	0	0	0	0	0	-	-
Spring	Bl	0	0	0	0	0	0	0	-	-
Spring	Ni	0	0	0	0	0	0	0	-	-
Spring	Gr	3	10	22	4	0	0	39	0.615	0.011
Summer	Br	0	0	0	0	0	0	0	-	-
Autumn	Os	0	0	0	0	0	0	0	-	-
Autumn	Gr	0	2	1	21	18	3	45	0.630	0.022
Winter	Ze	0	0	0	0	0	0	0	-	-
Winter	Kr	0	0	0	0	0	0	0	-	-
Winter	Pa	0	0	0	0	0	0	0	-	-
Winter	Br	0	0	0	0	0	0	0	-	-
Winter	Os	0	0	0	0	0	0	0	-	-
Winter	Bl	0	0	0	0	0	0	0	-	-
Winter	Ni	0	0	0	0	0	0	0	-	-
Winter	Gr	1	8	0	16	12	8	45	0.760	0.037
Total		4	20	23	41	30	11	129		
Accession number		AM180363	AM180364	AM180365	AM180367	AM180368	AM180366			

GD5

Season	Pop	D	E	R	D1	n	h	π
Spring	Ze	0	0	0	0	0	-	-
Spring	Kr	0	0	0	0	0	-	-
Spring	Pa	0	0	0	0	0	-	-
Spring	Br	0	0	0	0	0	-	-
Spring	Os	2	2	3	0	7	0.762	0.003
Spring	Bl	0	0	0	0	0	-	-
Spring	Ni	0	0	0	0	0	-	-
Spring	Gr	0	0	0	0	0	-	-
Summer	Br	0	0	0	0	0	-	-
Autumn	Os	0	0	0	0	0	-	-
Autumn	Gr	0	0	0	0	0	-	-
Winter	Ze	0	0	0	0	0	-	-
Winter	Kr	0	0	0	0	0	-	-
Winter	Pa	0	0	0	0	0	-	-
Winter	Br	0	0	0	0	0	-	-
Winter	Os	0	0	7	2	9	0.389	0.020
Winter	Bl	0	0	0	0	0	-	-
Winter	Ni	0	0	0	0	0	-	-
Winter	Gr	0	0	0	0	0	-	-
Total		2	2	10	2	16		
Accession number		AM180360	AM180361	AM180398	AM180399			

haplotype (F) did not occur in the center of this pattern. Finally, three rare haplotypes formed haplotype group Gd5, which was only observed in Os.

Unlike the parsimony network, the number of amino acid substitutions gave additional information on the relationship between the haplotype groups: no amino acid substitutions occurred between haplotype groups Gd1, Gd4a and Gd4b and between Gd2 and Gd5, while four – five amino acid changes occurred between groups Gd1+Gd4a+Gd4b, Gd2+Gd5 and Gd3. The number of unique fixed base differences (i.e. the number of bases at which a 'species' is different from all others, Kliman & Hey 1993) for the six groups ranged from 3 – 18.
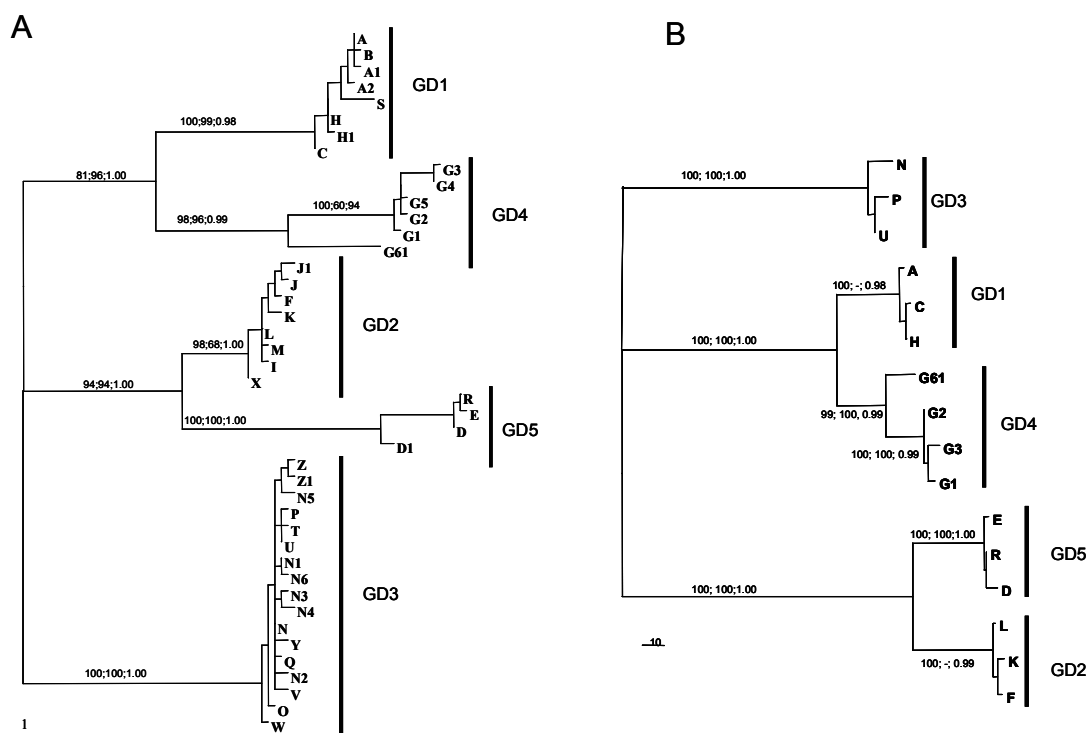
Fig. 4.4: *Geomonhystera disjuncta*. Maximum parsimony tree of COI haplotypes (A) and COI and ITS-spacer data combined (B). Five lineages (Gd1-5) are indicated with black bars. Bootstrap values of MP and NJ, followed by Bayesian probabilities are indicated above branches.

PHYLOGENETIC ANALYSIS

MP, NJ and Bayesian analysis of the 43 COI haplotypes yielded highly concordant tree topologies (Fig. 4.4a). Five haplotype groups with high bootstrap support and deep divergences were distinguished and were identical to five of the six subnetworks identified in the parsimony network (Fig. 4.3). Haplotype G61 (Gd4b) clearly was more related to the haplotypes of subnet Gd4a than to all other haplotypes.

The final ITS alignment was 749 bp long and contained 211 variable positions, 201 of which were parsimony informative. Up to four long indels (12 – 36 bp) were observed in the ITS1 alignment (338 bp), whereas four small indels (2 – 9 bp) occurred in the ITS2 alignment (247 bp). The 5.8S region (165bp) contained 0 – 25 substitutions, but no indels were observed. The partition homogeneity test suggested that COI and ITS did not possess significantly conflicting phylogenetic signals (p = 0.89). Both markers were therefore combined for further phylogenetic analysis and gave strong support for all five lineages (Fig. 4.4b). The total length of the ITS spacer region varied between the three major clades from 614 to 733 bp, while only few indel events were observed within each major clade (0 – 2 bp). Divergences within the five lineages varied between 0 – 2 %, while up to 22.9 % variation was present between lineages (Table 4.2). Interestingly, individuals containing the mitochondrial haplotype G61 had identical ITS sequences as individuals of lineage Gd4. We therefore divided all 759 individuals into five distinct lineages (taxa) (Gd1-5), and treated haplotype G61 as a long-branch within lineage Gd4. In addition, this subdivision is based on extrinsic geographical data (see next section). Adding G61 to Gd4 increased the intralineage divergence of the COI fragment to 10.9 %.

	GD1	GD2	GD3	GD4	GD5
GD1		17.6 - 23.2	23.6 - 25.4	17.36 - 19.3	22.1 - 23.2
GD2	19.8 - 21.1		20.6 - 23.2	21.2 - 25.7	13.8 - 16.1
GD3	19.5 - 21.1	22.4 - 24.1		21.9 - 25.4	24.4 - 25.7
GD4	1.0 - 1.2	19.5 - 19.6	18.9 - 20.8		22.8 - 25.1
GD5	20.0 - 20.3	3.4 - 3.7	22.9 - 24.7	19.8 - 20.0	

Table 4.2. *Geomonhystera disjuncta*. Divergence ranges (%) among the five lineages (Gd1-5). Above diagonal are values for the COI fragment, below diagonal are values for the ITS spacer region.

DISTRIBUTION OF THE FIVE GD LINEAGES

Fig. 4.1 shows the relative abundances and geographical distribution of each lineage at two (or three) sampling events. Several lineages co-occurred at different localities, but two were clearly restricted to one locality: Gd4 was only found in Gr and Gd5 in Os. Fig. 4.1 also indicates that Gd1 rather than Gd5 was dominant in Os. In fact, only 2 % of all individuals belonged to Gd5. In contrast, 43 % of all individuals belonged to Gd3.

Temporal fluctuations in relative abundances were especially prominent in lineage Gd2: more than 80 % of the individuals from Ni and Kr and more than 40 % of the specimens from Ze belonged to this group in April 2003. However, these abundances declined and even disappeared in January 2004, concomitantly with an increase in the relative abundance of lineage Gd3. Although Gd3 was highly abundant in the estuarine and coastal locations, it was not found in Os and Gr.

POPULATION GENETIC STRUCTURE

Values of intra-populational diversity parameters for each lineage separately are summarized in Table 4.1. Haplotype diversity (*h)* for each lineage was high and similar in all locations (Kruskal–Wallis: $p > 0.2$). Nucleotide diversity (π) was also similar among locations (Kruskal–Wallis: $p > 0.2$), but significant differences were observed when π values were compared between lineages ($p = 0.003$). These differences were situated between lineage Gd1 and Gd3 (Mann-Whitney U and corrected with Bonferroni: $p = 0.001$). Highest nucleotide diversity (π) was observed in populations of Gd4, but this was not significant after Bonferroni correction.

All sampled locations can freely exchange individuals, except for Os and Lake Grevelingen, which are isolated from the North Sea by man made barriers. Contrary to Lake Grevelingen, the Os population is not completely closed from the North Sea due to the presence of the storm surge barrier, which is open for several periods in a year.
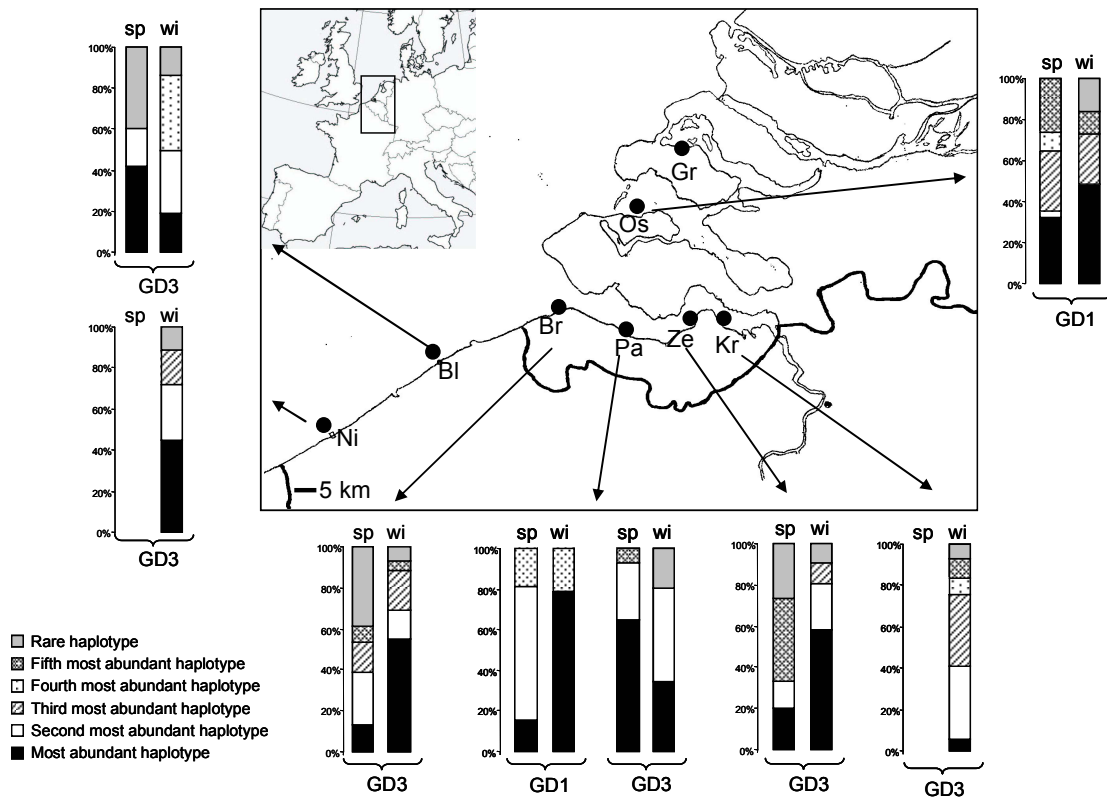
Fig. 4.5: *Geomonhystera disjuncta.* Lineage Gd1 and Gd3. Distribution of the five most abundant haplotypes of each lineage in spring 2003 (sp) and winter 2004 (wi) among the eight locations. Frequencies of haplotypes were summarized across the two seasons and all locations. Haplotypes A, H, C, S and B were the most abundant haplotypes for lineage GD1, respectively, and haplotypes N, U, V, N3 and Q for lineage GD3, respectively. All other haplotypes are pooled in a sixth class ('rare haplotypes'). Sample abbreviations are as in Fig. 4.1.

For Gd3, a highly significant structuring was observed even within the Westerschelde estuary, in April 2003 (Fst = 0.15, p < 0.0001) as well as in January 2004 (Fst = 0.13, *p* < 0.0001). In contrast, lineage Gd2 exhibited no significant genetic substructuring (Table 4.3). However, omitting Os did produce a low structuring among the other three locations (Fst = 0.056, p = 0.01). No correlation was found between DCE genetic distances and geographic distances (*p* > 0.5 for Gd1; *p* > 0.2 for Gd3), indicating that the observed genetic structure is not the result of an isolation-by-distance model.

	GD1			GD2			GD3		
	%	Fst	p-value	%	Fst	p-value	%	Fst	p-value
Spring 2003									
among populations	25.07	0.25	***	4.24	0.04	ns	13.20	0.13	***
within populations	74.93			95.76			86.80		
Winter 2004									
among populations	16.50	0.16	***				11.42	0.11	***
within populations	83.50						88.58		

Table 4.3. *Geomonhystera disjuncta*. Single- level AMOVA results for lineages Gd1, Gd2 and Gd3 in spring 2003 and winter 2004. (ns) not significant; (***) p < 0.0001.

TEMPORAL ANALYSIS OF POPULATION GENETIC STRUCTURE

The level of variation between populations (Fst values) did not change significantly over time (Fstat: $p = 0.56$ for Gd1, $p = 0.65$ for Gd3), but changes in the genetic composition among populations did occur (Manteltest, Gd1: $r = 0.44$ and $p = 0.1$; Gd3: $r = -0.12$ and $p = 0.73$). This change in haplotype composition is illustrated in Fig. 4.5 for both lineages. Because the frequency of lineage Gd1 was low in most locations (Table 4.1), only haplotype composition in Pa and Os are presented. Temporal differentiation was large and highly significant in Pa (Fst = 0.45), while only small differences were found in Os (Fst = 0.03). For Gd3, temporal differences were high in Ze (Fst = 0.2) and Bl (Fst = 0.11). No significant temporal changes were observed in Pa.

In addition, significant temporal fluctuations in haplotype frequencies were prominent for lineage Gd4 in Gr (Fst = 0.21, $p < 0.0001$), and for lineage Gd2 in Ni (Fst = 0.51, $p < 0.0001$). Temporal differentiation for lineage Gd5 in Os was high but only just significant (Fst = 0.15, $p = 0.03$).

DISCUSSION

MOLECULAR DIVERSITY IN NEMATODES

All our morphometric measurements fall within the range of variation observed in *G. disjuncta* (De Coninck & Schuurmans Stekhoven 1933, Hopper 1696) and several females contained eggs with embryos, a feature that within the genus only has been observed in *G. disjuncta* and *G. chitwoodi* (Chitwood, 1951). However, both species differ in the position of the vulva, which is situated much more posteriorly in *G. disjuncta*. Consequently, all specimens analysed in this study are *G. disjuncta*. Our morphometric data did not detect much morphological differentiation between lineages, but a more comprehensive study is clearly required to infer whether the genetic lineages are also accompanied by morphological differences.

Both COI and ITS data reveal high levels of molecular diversity within *G. disjuncta*: five distinct lineages were found on a small spatial scale, with low levels of divergence within lineages (< 3 %, except for Gd4), and high levels of variation between lineages (> 13 %). Intraspecific divergences for COI in parasitic nematode species are commonly lower than 5 % (Blouin 2002, Hu et al. 2002, Otranto et al. 2005), while congeneric species typically show divergences in the range of 10-20 % (Blouin 2002). However, a straightforward delineation of species based solely on genetic divergence data is problematic (Ferguson 2002): high levels of intraspecific divergence have been found in other nematode species, e.g. 8.4 % in *Oesophagostomum bifurcum* (de Gruyter et al. 2002) and 8.6 % in *Ancylostoma caninum* (Hu et al. 2002), while lower than 10 % divergence has been recorded between congeneric species of *Pellioditis* (Derycke et al. 2005) and *Ancylostoma* (Hu et al. 2002). Consequently, multiple molecular markers are needed for taxonomic interpretations of deeply diverged lineages within the Nematoda (Nadler 2002).

The ITS data reveal the same five lineages, but divergence values between them are much lower (< 4 %) than in the mitochondrial COI gene (> 13 %, see Table 4.2). Evolution of the ITS region is influenced by factors such as functional constraint, unequal crossing over and gene conversion, which all reduce intraspecific variation (Hillis & Dixon 1991). In addition, mitochondrial genes have higher mutation rates and a fourfold smaller effective size and consequently evolve more rapidly than the nuclear genes (Avise 2000).

POPULATION GENETIC STRUCTURE: SPATIAL AND TEMPORAL PATTERNS

Significant population structuring was observed in all lineages of *G. disjuncta* occurring at more than one location, even within the Westerschelde. This suggests restricted gene flow and limited effective dispersal between populations. However, observations of rafting (e.g. on algae, Derycke pers observ, and on sediment films, Faust & Gulledge 1996) indicate that dispersal in nematodes inhabiting algal substrata can be substantial (Ullberg 2004). Hence, it is questionable whether the observed genetic structure of the *G. disjuncta* lineages can be due to the mere lack of gene flow, as the exchange of only one migrant (assuming that selection and genetic drift are low, Slatkin 1987) could be sufficient to prevent the accumulation of large genetic differences between populations. Inspite of differences in life-history characteristics and habitat preferences, genetic structuring was similar in the most abundant lineage of the *P. marina* and *G. disjuncta* complexes: Fst values in April 2003 and Winter 2004 were 0.09 and 0.11, respectively, for PmI, and 0.13 and 0.11, respectively, for Gd3.

Our data also show that the observed genetic structure changes over time and that temporal fluctuations in haplotype frequencies are substantial within the *G. disjuncta* complex. *G. disjuncta* is a strong colonizer, which reaches its maximal abundances on decomposing algal thalli later and maintains high densities longer than *P. marina* (Bongers & Bongers 1998, Mokievsky et al. 2005, Derycke, unpubl. data). Hence, two alternative hypotheses for the differences in haplotype frequencies are plausible. First, the temporal differences can be caused by colonisation – extinction dynamics (De Meester et al. 2002, Derycke et al. 2006). Considering the ephemeral nature and patchy distribution of algal deposits, metapopulation dynamics are indeed likely in *G. disjuncta*. However, *G. disjuncta* is also frequently observed in the sediment, and consequently extinction of *G. disjuncta* when algae are completely decomposed is unlikely. Another explanation is that *G. disjuncta* colonizes the algae and subsequently exhibits priority effects, i.e. the first colonising individuals have such a strong population development that they reduce the settlement of new specimens. Depending on which individuals arrive at the patches, differences in haplotype composition can occur. Such priority effects have been observed in lenthic habitats (Boileau et al. 1992) and recently also in a field experiment with *P. marina* (Derycke et al. 2007c).

TAXONOMY IN MARINE NEMATODES

Both COI and ITS data reveal high levels of intraspecific diversity within *G. disjuncta*. The concordance among COI and ITS data suggests cyto-nuclear disequilibrium, which is caused by either reproductive isolation, epistatic effects across genomes or drift (Asmussen et al. 1987). Even separately (i.e. ITS1, ITS2 and to a lesser extent 5.8S, data not shown), the nuclear regions show the same phylogenetic pattern as the mitochondrial gene, hence the disequilibrium is most likely caused by reproductive isolation (Latta et al. 2001). In addition, the number of unique fixed differences between lineages for both molecular markers confirms that all lineages have distinct gene pools, even though they co-occur at most locations. Both arguments suggest that the lineages are in fact 'biological species'. As all lineages are monophyletic for both molecular markers, they are also phylogenetic and genealogical species (Rocha-Olivares et al. 2001). Lineage Gd3 contains the highest number of haplotypes and is the most abundant and widespread lineage. It has, however, the lowest nucleotide diversity of all lineages, indicating that haplotypes have not accumulated many mutations. Several unique haplotypes are present and connected via a star-like pattern, which suggests a recent radiation of this lineage (Rogers & Harpending 1992).

Two pairs of sistertaxa are present (Gd1 and Gd4, Gd2 and Gd5), with Gd4 and Gd5 exclusively found in Gr and Os, respectively. As elaborately described and discussed in Derycke et al. (2006), allopatric speciation is unlikely since the geographical separation happened too recently for the lineages to have accumulated such high divergences. However, Ullberg (2004) pointed out that restricted gene flow and the direct developing larvae in nematodes can lead to an increased speciation rate in this phylum. Next to the presence of geographical barriers in both Os and Gr, they also contain different environmental characteristics and substrata (Derycke et al., 2006). Clearly, additional sampling in Gr and Os and on a broader geographical scale is needed to elucidate the modes of speciation.

The cryptic diversity observed in *G. disjuncta* as well as in *P. marina* highlights the difficulties of a morphology-based identification system for nematodes. In view of the effort required to find morphological diagnostic features, DNA-barcoding may provide a first step towards a more efficient search (De Ley et al. 2005). The COI gene has been designated as a good marker for barcoding life on earth

(Hebert et al. 2003a,b), and at first sight, the results of the present and earlier work (Derycke et al. 2005, 2006) could be considered as an indication that COI would be applicable for nematode identification, as it recognizes both cryptic and morphological taxa. Moreover, a huge part of the nematode diversity is currently unknown, and therefore a good barcoding marker for the phylum Nematoda preferably should also be phylogenetically informative so that new species can be discovered. Our COI sequences were only moderately phylogenetically informative, and some haplotypes remained unresolved (e.g. haplotype G61, or the Z haplotypes in *P. marina*, Derycke et al. 2006), supporting the contention that more than one genomic DNA sequence is required to distinguish closely related taxa by barcoding (Mallet & Willmott 2003, Tautz et al. 2003). One major drawback of the COI gene is its difficult amplification within the Nematoda (De Ley et al. 2005, Derycke et al. 2005, Bhadury et al. 2006). This and previous studies (Derycke et al. 2005, 2006) illustrate that more than one set of primers will be required for COI barcoding in this phylum. The ITS fragment, by contrast, was easily amplified in our species, but we feel that it is not a good universal identification tool for two reasons: 1) intra-individual variation was frequently observed, which reduces the sequencing signal and 2) a high amount of indel events are present within closely related cryptic taxa, rendering alignment between divergent taxa problematic. A promising alternative for DNA barcoding purposes in closely related nematode groups for which COI was not a good marker may be the SSU and LSU rDNA segments (Floyd et al. 2002, Blaxter 2004, De Ley et al. 2005), which also works well for *P. marina* (Chapter 6 and 9).

CONCLUSION

Our studies in two nematode species (*G. disjuncta* and *P. marina*) indicate that cryptic diversity is likely to be substantial within free-living nematodes. This has important implications for biodiversity studies, and potentially renders a highly speciose phylum even more speciose than anticipated. Differences in life-history characteristics between *P. marina* and *G. disjuncta* did not result in clear differences in genetic patterns. Furthermore, colonisation dynamics in combination with persistent founder effects were the most plausible explanation for the observed genetic patterns within the *G. disjuncta* lineages. In addition, *P. marina* and *G. disjuncta* prevail on decomposing macroalgae in estuaries and coastal zones. Because of their life-history characteristics and 'epiphytic' rather then benthic microhabitats, they are not very typical marine nematodes. Therefore, extrapolation of our results to other marine nematodes requires some caution. Further research on a truly marine, less opportunistic species with different habitat preferences and life-history characteristics than *P. marina* and *G. disjuncta* will provide information on the generality of our results for the Nematoda. Such information is crucial to any assessment of marine nematode species diversity and to barcoding attempts for the phylum Nematoda in general.

ACKNOWLEDGEMENTS